TÜBİTAK

Turkish Journal of Chemistry

http://journals.tubitak.gov.tr/chem/

Research Article

Turk J Chem
(2022) 46: 1504-1515
© TÜBİTAK
doi:10.55730/1300-0527.3455

Schiff base containing pyridine groups functionalized water-soluble phthalocyanine: Synthesis, photo-physicochemical properties, and bovine serum albumin binding behavior

Öznur DÜLGER KUTLU, Ali ERDOĞMUŞ*
Department of Chemistry, Yıldız Technical University, İstanbul, Turkey

Received: 28.01.2022 • **Accepted/Published Online:** 20.05.2022 • **Final Version:** 05.10.2022

Abstract
The novel pyridine bearing schiff base substituted metal-free (**9**), zinc(II) phthalocyanine (**10**), and its quaternized derivative (**11**) were designed and synthesized. These phthalocyanines were fully characterized by spectroscopic methods (FT-IR, UV–Vis, MALDI-TOF, and ^{1}H NMR). The photo-physicochemical properties of these phthalocyanines were investigated in both DMSO and DMF for **10** and in both DMSO and aqueous solution for **11**. The addition of pyridine bearing Schiff base groups as peripheral ligands showed an improvement in the photophysical and photochemical properties. In addition, a spectroscopic investigation of the binding behavior of the water-soluble zinc (II) phthalocyanine complex to bovine serum albumin (BSA) was also studied in this work.

Key words: Photochemistry, photophysics, water-soluble phthalocyanine, pyridine group

1. Introduction

Phthalocyanines (Pcs) settled of four isoindole units bonded by azomethine bridges are considerable tetrapyrrolic macro heterocyclic compounds with a delocalized 18-π electrons system [1–3]. Pcs attract considerable attention in the scientific world due to their ability to complex with many metals in the periodic table [4], to change their chemical and physical properties according to the metal atom and substrate used in complex formation, and to have unique electronic, magnetic and optical properties [5–7]. Thanks to these properties, phthalocyanines, and their derivatives are used in optical data storage and optoelectronics [8–10], aggregates and organic polymers in dye-sensitive solar cells (DSSC) [11,12], light-emitting diodes [13,14], gas sensors [15], coordination bonding, where catalysis with redox properties is required and in the manufacture of liquid crystals [16], they are also used in many different fields such as the production of conductors [17], electrochromic imaging [18], photocatalysts [19], and water splitting [20]. In addition, these compounds can be used as photosensitizers in photodynamic therapy applications due to easy design, nontoxic geste in dark, and strong absorption in the therapeutic window [21,22]. The photophysical and photochemical properties of phthalocyanines are largely dependent on the central metal ion. Complexes formed with diamagnetic metal ions such as Ga^{3+}, Si^{4+}, and Zn^{2+} help to obtain high quantum yields and long lifetime compounds in the exciting ternary state, which are necessary for the activity of PDT [23]. The low solubility of Pcs in water and other organic solvents and the increased aggregation tendency limit their use in PDT applications. [24]. However, the substitution of Pcs rings with –COOH, SO_3H, and quartenized amino groups can increase their solubility in water and/or organic solvents. In PDT applications, the drug is administered straight into the person's bloodstream which is a hydrophilic system, hence, it becomes more important that the photosensitizer is soluble in water [25,26].

Pyridine derivatives are important intermediates with excellent biocompatibility, which can create hydrogen bonds with biological macromolecules thanks to basic nitrogen atoms [27]. By quaternizing the amino group, macro rings with high water solubility are obtained. Schiff bases are a significant class of organic compounds, and the imine groups in these compounds are critical to their biological activity [28]. There is limited study on Pcs containing Schiff base for different applications [29], especially their photochemical and photophysical features [30]. This study aims to design water-soluble phthalocyanine complexes bearing Schiff base and pyridine groups and investigate spectroscopic and photo-physicochemical properties of the molecules to show their efficiency in PDT applications. The results are compared with

* Correspondence: aerdog@yildiz.edu.tr

This work is licensed under a Creative Commons Attribution 4.0 International License.

other zinc phthalocyanine containing Schiff base complexes from the literature [29–32]. Bovine serum albumin (BSA) is one of the major plasma proteins that contributes significantly to physiological functions and exhibits effective drug-delivery roles [33,34], hence the investigation of the drugs binding with BSA is of interest. The binding behaviour of the quaternized zinc phthalocyanine (**11**) to BSA protein was also investigated in this work.

2. Experimental

The experimental parameters (materials, equipment, synthesis, characterization data, photo-physicochemical formulas, and photo-physicochemical measurement conditions) were given in the supporting information.

2.1. Binding properties of the quaternized zinc(II) phthalocyanine to BSA protein

The formulas and measurement conditions used to determine the BSA protein binding properties of the quaternized zinc (II) phthalocyanine were given in the supporting information.

3. Results and discussion

3.1. Synthesis and characterization

The chemical synthesis pathway to the complexes used as a starting compound from **2** to **7** is described in Scheme 1. The metal-free phthalocyanine bearing acetal group (**4**) was obtained by treatment of the related phthalonitrile derivative (**3**) in the presence of DBU catalyst in n-pentanol at reflux temperature under argon atmosphere. The metal-free phthalocyanine bearing aldehyde group (**6**) was obtained by applying the acetal deprotection method to **4** in the acetic acid/$FeCl_3$ protection system according to the published procedure [35]. The acetal and aldehyde substituted zinc (II) phthalocyanines (**5** and **7**) were obtained by treatment of the related metal-free acetal and aldehyde phthalocyanines (**4** and **6)** in the presence of anhydrous $Zn(CH_3COO)_2$ as a metal source in anhydrous n-pentanol.

The novel Schiff base substituted metal-free (**9**), zinc (II) (**10**), and water-soluble zinc (II) phthalocyanines (**11**) were obtained by treatment of the related phthalocyanine **4** using as a starting material (Scheme 2). The Schiff base-substituted H_2Pc (**9**) was obtained by the condensation reaction between complex **6** and 4-aminomethyl pyridine (**8**). Then, the novel compound **10** was obtained by the reaction of compound **9** with anhydrous $Zn(OAc)_2$ in the presence of DBU in n-pentanol. New quaternized zinc (II) phthalocyanine **11** was synthesized by the reaction of **10** with dimethyl sulfate which was used as a quaternization agent [24].

The structures of the starting compounds **2** and **3** were synthesized according to the published procedure [35] and all synthesized compounds were characterized by different spectroscopic methods. The FT-IR spectrum showed the formation of **2** due to the characteristic vibrations corresponding to the -C ≡ N vibrational band at 2238 cm^{-1}, the ether group (Ar-O-Ar) at 1257 cm^{-1}, as well as tension vibrations at 1691 cm^{-1} that corresponds to the carbonyl group (-C = O). The FT-IR spectrum of **3** showed specific bands at 2956, 2888 cm^{-1}, and 1205, assigned to C-H, and C-O-C respectively. After the conversion of phthalonitrile **3** to **4**, the monitored -C ≡ N vibration of **3** disappeared, and the -NH band of metal-free phthalocyanines appeared at 3288 cm^{-1} (Figure S1). In the FT-IR spectrum (Figure S2) of acetal-ZnPc (**5**), the disappearance of the -NH vibration peak of compound **4**, aliphatic CH vibrations at 2951, 2881 cm^{-1}, and C-O-C vibrations at 1107 cm^{-1} support the formation of compound **5**. The disappearance of the C-O-C vibrational band for the acetal group in the FT-IR spectrum of compound **4** and the appearance of a new -C=O group vibration band observed at 1693 cm^{-1} proved the formation of phthalocyanine **6** (Figure S4). The disappearance of the –NH vibrational band for metal-free phthalocyanine in the FT-IR spectrum of compound **6** proved the formation of phthalocyanine **7** (Figure S4). Vibrations belonging to the –N=CH– stretching band were observed at 1642 cm^{-1} (Figure S5) for **9**. Concerning the FT-IR spectra of **10** (Figure S6), the disappearance of the -NH vibration verified the formation of the designed compound **10**. The appearance of a new vibrational band (aliphatic C-H vibrations) (Figure S7) caused by the quaternization was observed at 2959–2862 cm^{-1} and verified the formation of the quaternized ZnPc **11**.

The ^1H NMR results supplied acceptable data about the proposed configurations of the designed complexes. The relative ^1H-NMR spectrum of compounds (**2**, **3**, **5,** and **7**) was consistent with the previously published article [35]. In the ^1H NMR spectra of **3**, the acetal protons were observed at 5.56 ppm and the aromatic protons at 7.50–6.60 ppm. In the ^1H NMR spectrum of **6**, the appearance of the aldehyde protons at 10.05–10.00 ppm was evidence for the formation of the described compound. The peak of the azomethine proton, one of the characteristic peaks of these compounds in the ^1H NMR spectra of Schiff bases, usually resonates in the range of 8–9 ppm. In the ^1H NMR spectrum of complex **9**, the signals of the azomethine group and the pyridine group were detected in the range of 8.73–8.68 ppm and 4.90–4.85 ppm, respectively and confirming the formation of **9** (Figure S8). The -NH peaks belonging to the H_2Pc ring were not observed. The presence of signals belonging to the pyridine on the phthalocyanine macrocycle, observed at 9.66 and 8.41 ppm (Figure S9), was evidence for the formation of the **10**, according to the literature [36].

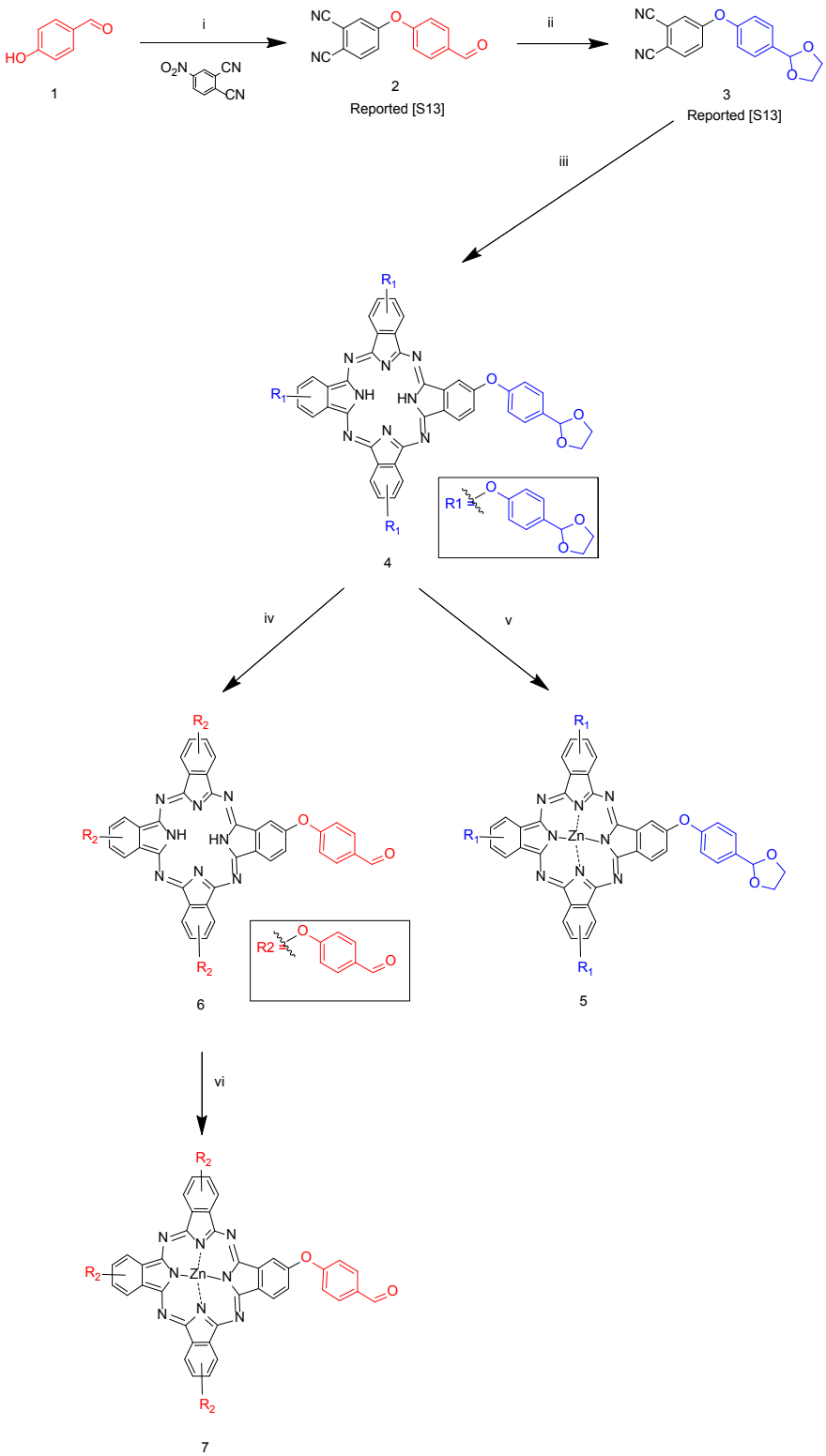

Scheme 1. The synthesis pathways of components used as starting material from **2** to **7**. Reaction conditions: i) K_2CO_3, DMF, rt, 24 h; ii) ethylene glycol, PTSA, toluene, 110 °C, 48 h; iii) n-pentanol, DBU, 140 °C, 18 h; iv) THF, acetic acid, $FeCl_3 \cdot 6H_2O$, rt, 24 h; v) $Zn(OAc)_2$, n-pentanol, 140 °C, 18 h; vi) $Zn(OAc)_2$, n-pentanol, 140 °C, 18 h.

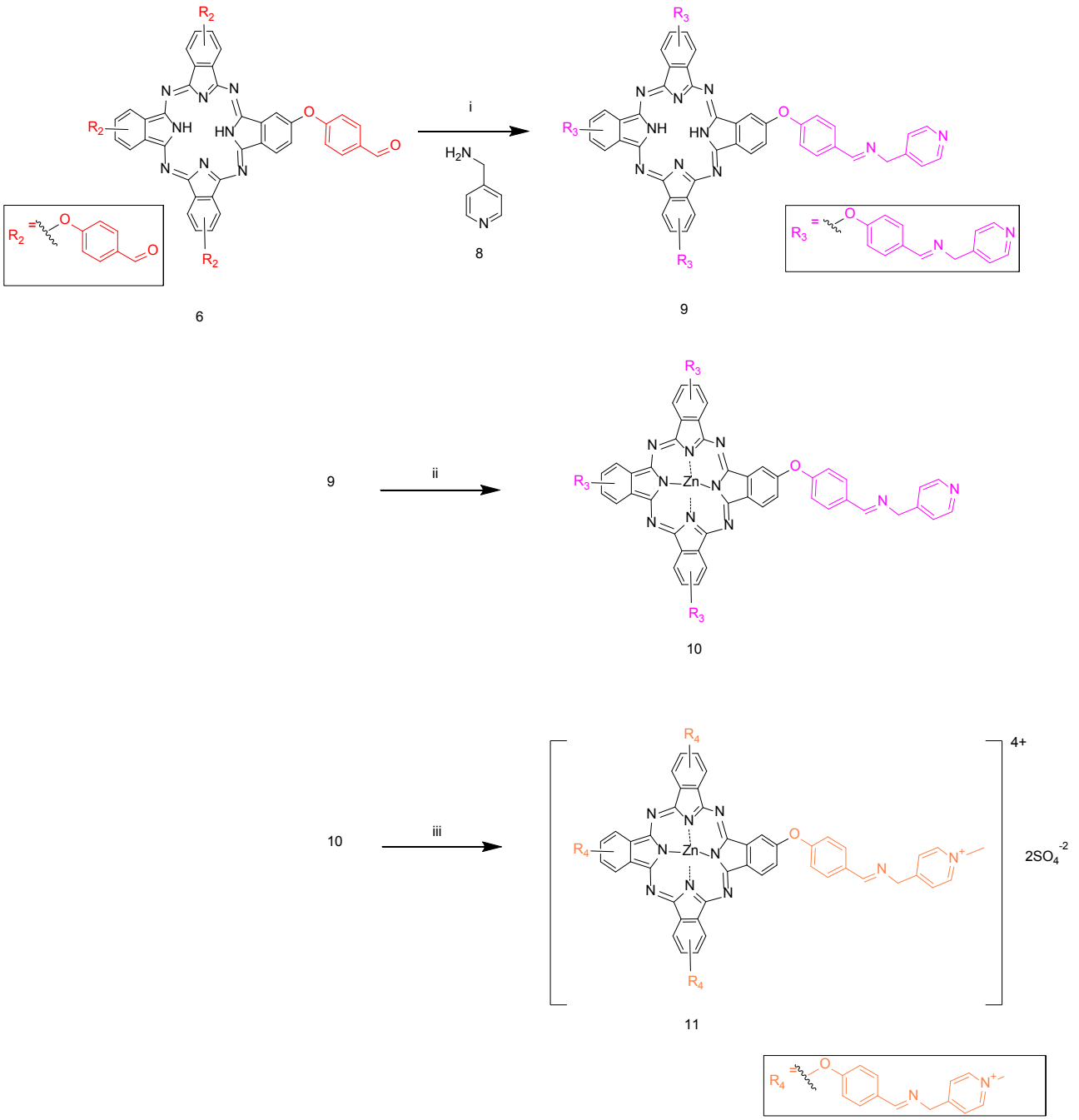

Scheme 2. Synthesis of the imine containing Schiff base-substituted metal-free, zinc (II), and quaternized zinc phthalocyanines. Reaction conditions: i) DCM, 35 °C, 20 h; ii) $Zn(OAc)_2$, n-pentanol, 140 °C, 18 h; iii) Dimethyl sulphate, 120 °C, 12 h.

In the ^{1}H NMR spectrum of the quaternized complex **11**, the –CH_3 protons were observed as a singlet peak at 4.28 ppm (Figure S10), identifying the formation of the quaternized product. These results confirmed the structure of compound **11**. In addition to ^{1}H NMR spectrum results, the MALDI-TOF MS data for the substituted metal-free (**4**, **6**, and **9**), zinc phthalocyanines (**5**, **7,** and **10**), and the quaternized derivative **11** are available for the formulations given. The molecular ion peaks of synthesized Pcs showed parent ions at m/z: 1170.336 as $[M]^+$ for **3**, 1056.094 $[M+K+Na]^+$ for **4**, 1236 $[M+2H]^+$ for **5**, 1057.91 $[M+H]^+$ for **6**, 1355.288 $[M]^+$ for **7**, 1418.10528 $[M]^+$ for **8**, 1939.192 [M+ DIT+K+3H]$^+$ for **9**, respectively (Figure S11a–S11e). The molecular ion peak values of the fragmentation products of the obtained complexes are also indicated in the supplementary file.

3.2. Photophysical and photochemical studies

3.2.1. Ground state electronic absorption spectra and aggregation studies

The ground state electronic absorption spectra of phthalocyanines and their metal derivatives in the studied solution are one of the principal pieces of evidence for their formation. The newly synthesized phthalocyanines for H_2Pc (**4**, **6**, and **9**) and metallophthalocyanines (**10** and **11**) are detected by the characteristic Q- and B-bands in their electronic spectra. The electronic spectral properties of phthalocyanines, determined by the 18π system of the innermost 16-membered ring, form the basis of their chemical and electrical properties that metal-free phthalocyanine compounds with D_{4h} symmetry corresponding to the π→π* transitions show a single absorption, while nonmetallic phthalocyanines with D_{2h} symmetry show two absorptions with equal intensity in the same range [37]. The UV–vis spectrum of H_2Pc **4**, **6** in DMSO and **9** in DMSO and DMSO (plus Triton X-100) and DCM (as an example for **11)** was given in Figure S12, its zinc derivative **8** in DMSO and DMF, quaternized zinc derivative **11** in DMSO and water (Figure S13), were recorded at room temperature. The logarithmic molar absorption coefficient values of the bands are listed in Table 1. In DMSO, the two characteristic absorption bands at Q band region of the metal-free phthalocyanines were observed at 669 and 664 (Qx and Qy) nm for **4**, 699 and 666 nm for **6**, and 700 and 669 nm for **9**, respectively (Figure S13) (Table 1). However, the B-bands for all H_2Pc compounds were seen between 330 and 355 nm.

DMSO is known as a strong coordination solvent that prevents aggregation. However, aggregation was observed for **4**, **6**, and **9** in DMSO. Figure S12 showed that the addition of Triton X-100 to the medium did not affect the solubility though it decreased the aggregation tendency of **9** in the solvent. The UV–vis spectra of the metal free phthalocyanine (**9**) showed two characteristic absorption bands at Q band region around 697 nm and 672 nm in DCM solution. It was observed that the solubility of **9** increased in the absorption spectra in DCM solution, it was not effective on the decrease of aggregation tendency and solubility in DMSO.

The electronic spectra of ZnPc **10** and quaternized ZnPc **11** showed characteristic absorption bands at around 685–707 nm and 320–370 nm for the Q band and the B band regions which are characteristic of metallophthalocyanines in DMSO (Table 1) [38].

The characteristic single absorption band of zinc phthalocyanines for **5**, **7**, and newly synthesized **8** was observed at 677 nm, 676 nm, and 675 nm in DMF, respectively (Figure 1, Table 1). The absorption spectra of the quaternized complex **11** showed a co-surface aggregation in water, as evidenced by the presence of two bands in the Q band region (Figure 2). These bands appeared at 675 nm (weak) due to monomeric species and low energy (redshifted) at 638 nm (Table 1) due to aggregate species. The incorporation of **11** in water with quantities of TX-100 causes a sharpening of the absorption band at 680 nm, which clearly shows the decrease of aggregation after the interaction of the host-guest by the addition of surfactant [39].

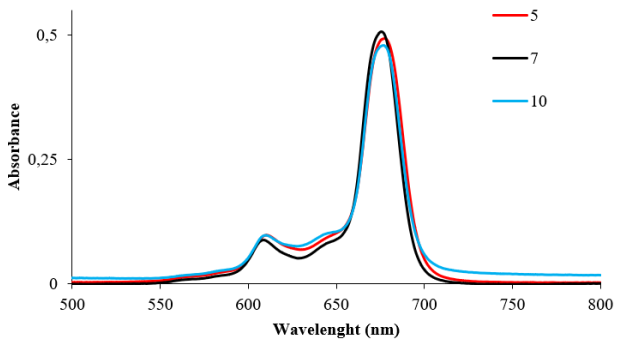

Figure 1. The absorption spectra of ZnPcs **5**, **7,** and **10** in DMF (concentration 6.0 × 10^{-6} M).

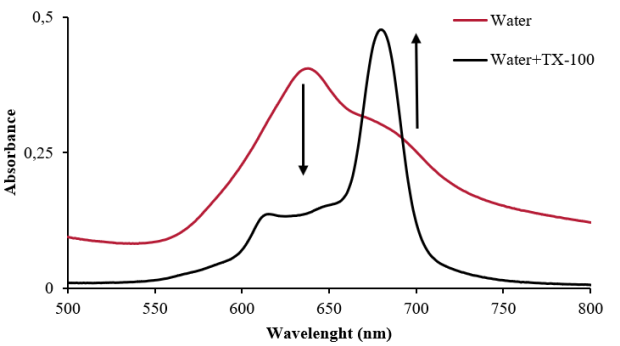

Figure 2. The absorption spectra **11** in water solution before and after the addition of TX-100.

The aggregation behavior of Pc is usually represented as a coplanar relationship of oriented rings from monomer state to dimer state and depends on many variables (such as concentration, solvent and nature of substituents, metal ions, and temperature) [40]. For the metal phthalocyanines, aggregation is often undesirable as it decreases photoactivity [41].

The aggregation behavior of the compounds was studied in DMSO and DMF for **5**, **7**, and **10** and in water with quantities of TX-100 and DMSO for **11**. After the addition of some drops of TX-100 to the aqueous solution of compound **11**, the Q band at about 640 nm was observed to shift to 680 nm (Figure 2), which are lower energy for compound **11**. However, as shown in Figure 2, the addition of TX-100 did not completely inhibit the aggregation of **11** in water. Comparing the UV-vis spectra of zinc phthalocyanine **11** in water and DMSO (Figure S13), it was observed that it exhibited lower aggregation in DMSO, which has a lower polarity than water, while it exhibited an H-type aggregation in water [42].

The Beer-Lambert law was followed for all of these complexes at concentrations ranging from 2×10^{-6} to 12×10^{-6} M. The results showed that ZnPcs (**5**, **7**, and **10**) (in DMF and DMSO) (as an example for **10**, in DMSO and DMF was given in Figure 3 and Figure S14) and the quaternized derivative of ZnPc **11** in DMSO (Figure 3) did not display aggregation.

3.2.2. Fluorescence spectra

Fluorescence properties of the synthesized phthalocyanine compounds (**5**, **7,** and **10**) were investigated in DMSO and DMF, the quaternized metallophthalocyanines **11** in water containing TX-100, and DMSO. The absorption, fluorescence emission, and excitation spectra of complexes **10** in DMSO and **11** in water containing TX-100 are shown in Figure 4 as an example. Fluorescence emission peaks are also listed in Table 1.

Table 1. Spectral parameters of **4**, **5**, **6**, **7**, **9, 10,** and **11** in different solvents.

Comp.	Solvent	Q band λmax, (nm)	log ε	Excitation λ_{Ex}, (nm)	Emission λ_{Em},(nm)	Stokes Shift Δ_{Stokes}, (nm)
4	DMSO	669,664	-	-	-	-
5	DMSO[33]	679	5.04	681	691	12
	DMF	677	5.60	678	689	12
6	DMSO	699,666	-	-	-	-
7	DMSO[33]	678	5.24	679	690	12
	DMF	676	5.77	676	687	11
9	DMSO	700,669	-	-	-	-
	DCM	697,672	-	-	-	-
10	DMSO	679	5.00	681	693	14
	DMF	675	4.77	676	688	13
11	DMSO	679	4.89	681	693	14
	water+TX-100	680	4.62	683	692	12

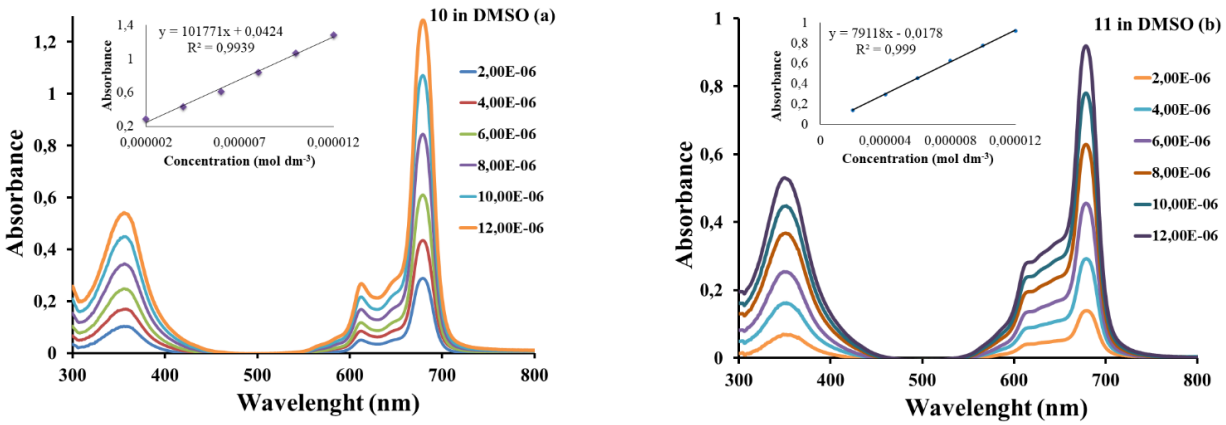

Figure 3. The absorption spectra of complexes **10 (a)** and **11 (b)** in DMSO at different concentrations.

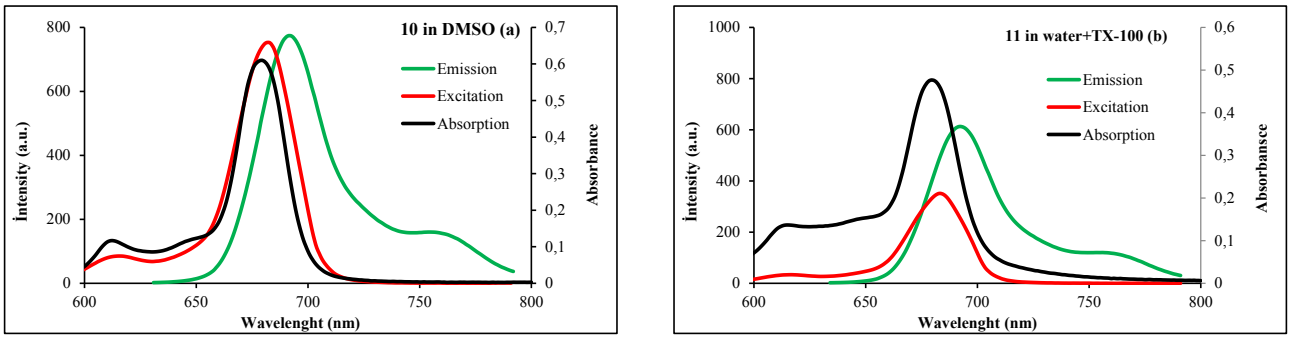

Figure 4. Absorption, excitation and emission spectra of the phthalocyanines **10 (a)** in DMSO and **11 (b)** in water containing TX-100.

The Stokes shifts of ZnPc complexes were observed in the ~10–14 nm range. The ZnPcs (**5**, **7,** and **10**) indicated similar fluorescence behavior in DMF and DMSO. The excitation and absorption spectra were similar to each other and were both mirror images of the fluorescence spectra for complexes (**5**, **7**, and **10)** in DMSO and DMF. Hence, these results suggested that the nuclear configurations of the ground are similar to the excited states and are not affected by the excitation of ZnPcs. In water media, while complex **11** was not fluorescent property due to high aggregation tendency it showed fluorescence property in DMSO. Also, 9 did not give emission in the studied organic solvents due to its aggregation. Since aggregation has no emission behavior, the emission properties of compounds with high aggregation tendency in the solutions are very low or not observed [43].

3.2.3. Fluorescence quantum yields

Fluorescent molecules have recently gained importance in PDT applications, as they provide the opportunity to monitor how they progress in the body and whether they accumulate in cancer cells. For this reason, the fluorescence properties of photosensitizers **5**, **7**, and **10** were investigated. In addition, due to the low solubility of Compounds **4**, **6**, and **9** in DMSO and DMF solvents and their high aggregation tendency, the fluorescence properties of these compounds could not be investigated. Table 2 shows the Φ_F of ZnPc complexes (**5**, **7**, and **10**) in DMSO and DMF and for the quaternized ZnPc **11** in both DMSO and water containing TX-100. The fluorescence quantum yield (Φ_F) value of the newly studied zinc Pc complex **10** was slightly lower than the unsubstituted zinc Pc (Φ_F = 0.20) in DMSO and was also lower than its quaternized derivative **11** substituted with quaternized imine conjugated pyridine group in aqueous media [44]. The quaternized complex **11** had a high Φ_F value in water (plus 0.1 mL TX-100) compared to DMSO due to the aggregation in the first solvent. The fluorescence quantum yield of the Schiff base substituted complex **10** was not significantly increased compared to compounds **5** and **6** according to the literature [31].

As shown in Table 2, Φ_F of **5**, **7**, and **11** in DMF are higher than those for standard ZnPc (Φ_F = 0.17) [42]. The novel compound **10** showed a lower Φ_F value in DMF compared to zinc phthalocyanines (**5**, **6**) in the same solution (DMF) (Table 2).

3.2.4. Singlet oxygen quantum yields

Singlet oxygen causing irreversible destruction of cells within the irradiated tumor area is a measure of the effectiveness of the PDT procedure. The amount of singlet oxygen produced is the most important indicator of using it as a photosensitizer. Singlet oxygen quantum yield (Φ_Δ) is a measure of singlet oxygen generation efficiency and the Φ_Δ values were obtained using Eq. (5) (given Sup. File). Information about the singlet oxygen measurement conditions was given in the supplementary file. Singlet oxygen quantum yields were studied in organic solvents (DMSO and DMF) for the studied ZnPcs (**5**, **7**, **10**) using 1,3-Diphenylisobenzofuran (DPBF) as a quencher and water (plus 0.1 mL TX-100) for the quaternized ZnPc **11** using 9,10-anthracenediyl-bis(methylene)dimalonic acid (ADMA) as a quencher. The disappearance of DPBF or ADMA was monitored using a UV-vis spectrophotometer in Figure 5 (a) using DPBF in DMSO and Figure 5 (b) using ADMA in water plus TX-100 for complex (**11**). The Φ_Δ values of the studied Pcs (**5**, **7**, **10,** and **11**) and standard ZnPc are listed in Table 2. There were no changes in the intensities of the Q band absorptions of the ZnPc derivatives during the Φ_Δ determination process.

The Φ_Δ value of ZnPc Schiff base bearing **10** was found to be 0.78 in DMSO. This value of **10** was higher than the ZnPc Schiff base bearing in the literature [30,31] and Std-ZnPc (Φ_Δ = 0.67). Comparing DMSO and DMF, the Φ_Δ value of ZnPc **10** in DMSO is higher than in DMF. This situation may have resulted from the amine group's attempt to quench the singlet oxygen in DMF. The novel ZnPc (**10**) bearing the Schiff base produced higher singlet oxygen generation in DMF with a Φ_Δ value of 0.64 compared to the Std-ZnPc (Φ_Δ = 0.57), ZnPcs **5** (Φ_Δ = 0.58) and **6** (Φ_Δ = 0.62). According to these results, the presence of Schiff base as a ligand increases the Φ_Δ with the increase of intersystem transition [46,47].

The fact that ZnPc **10** has a higher Φ_Δ value than its quaternized form **11** in DMSO suggests that the quaternization of ZnPc complexes causes a decrease in Φ_Δ values. In addition, Table 2 shows that low Φ_Δ values were observed for **11** in water containing TX-100 compared to DMSO. The absorption of both singlet oxygen and water around 1270 nm has a great effect on the lifetime of singlet oxygen. This explains why the Φ_Δ value in water is lower than the one in deuterated water and DMSO [46]. Φ_Δ of **11** showed higher than singlet quantum yields compared to previously studied quaternized zinc analogs bearing the pyridine group in DMSO [42].

3.2.5. Photodegradation quantum yields

Photodegradation is a photochemical method used to determine the stability of phthalocyanines under the influence of applied light which is critical for molecules designed for use as photosensitizers in PDT. It is expected that the concentration of the drug molecule used in photocatalytic applications such as PDT will not change during the treatment process, that is, it will be stable. The photodegradation quantum yield (Φ_d) values for the complexes listed in Table 2 are of the order of 10^{-4}. Stable ZnPc molecules showing Φ_d values between 10^{-6} and 10^{-3} have been reported [48]. The change in the absorbance values observed in the Q-band during the Φ_d measurement of **10** and **11** in DMSO is presented in Figure 6. The synthesized compounds were found to be less stable than standard ZnPc in DMSO (0.26×10^{-4}) and DMF (0.23×10^{-4}) [45]. Compared with the photodegradation quantum yields of compounds **5** and **6**, an increase in the photodegradation quantum yields in DMSO and DMF was observed with the incorporation of imine bond-conjugated pyridine groups into the structure.

When the pyridine substituted phthalocyanines were in terms of solvent effect, it was seen that the stability in DMSO was higher than that of DMF. Quaternization of pyridine groups caused a decrease in the stability of the ionic zinc Pc complex **11**. Compound **11** is less stable in water containing TX-100 (Figure S15) than in DMSO.

3.2.6. Binding properties of quaternized zinc(II) phthalocyanine to BSA protein

Bovine serum albumin (BSA), is the predominant protein in the blood, it has a very important role in the delivery of drugs. One of the studies to determine drug delivery to specific tissues through the bloodstream is the analysis of the BSA binding properties of photosensitizers [49,50]. Accordingly, the binding properties of the novel quaternized ZnPc **11** to BSA protein were investigated by spectrofluorometric at room temperature in PBS [51] in an aqueous solution. The PBS of a fixed concentration of BSA (3.00×10^{-5} M) was titrated with varying concentrations of the **11** solution. BSA was excited at 280 nm and the fluorescence emission spectra were reported between 290 and 500 nm for compound **11**-BSA solution. The fluorescence emission peak of BSA at 348 nm decreased by increasing the phthalocyanine concentrations due to the interaction of the phthalocyanine molecules with the tryptophan residues on the BSA protein (Figure 7).

When the fluorescence quenching studies of water-soluble ZnPc and BSA in the literature [51–53] were examined, it was understood that compound **11** was more effective in the fluorescence quenching of BSA. The Kq value was obtained for **11** and as shown in Table 3, the fact that the value of kq (0.97×10^{13} M^{-1} s^{-1}) is higher than the recommended value for dynamic quenching (10^{10} M^{-1} s^{-1}) [53] indicates that the quenching mechanism is static. A bimolecular quenching constant (Kq) of **11** was acquired by Equation (6) (in supplementary file) using an approximate fluorescence lifetime of BSA [54]. In fluorescence quenching of **11** by BSA in PBS, Stern-Volmer kinetics consistent with diffusion-controlled bimolecular reactions were investigated. The fluorescence emission changes in BSA upon binding of complex **11** are observed in Figure 7. The slope of the graph demonstrated in Figure 7 gave the Stern–Volmer constant (K_{SV}) value indicated in Table 3.

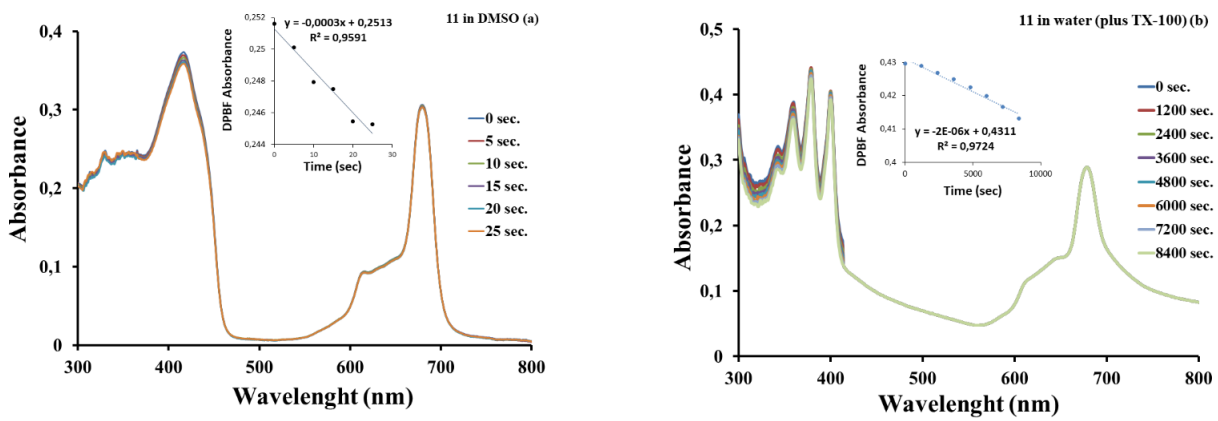

Figure 5. A typical spectrum for the determination of singlet oxygen quantum yield of the complex **11** in DMSO (a) and in water (plus 0.1 mL TX-100) (b).

Table 2. Photophysical and photochemical parameters of **5, 7, 10** and **11** in DMSO, DMF, and water (plus TX-100).

Compound	Solvent	Φ_F	Φ_d (10^{-4})	Φ_Δ
5	DMSO[33]	0.08	1.0	0.68
	DMF	0.23	3.08	0.58
7	DMSO[33]	0.11	0.61	0.78
	DMF	0.25	9.11	0.62
10	DMSO	0.12	0.82	0.78
	DMF	0.19	11.0	0.64
11	DMSO	0.28	2.01	0.66
	water+TX-100	0.14	24.03	0.14

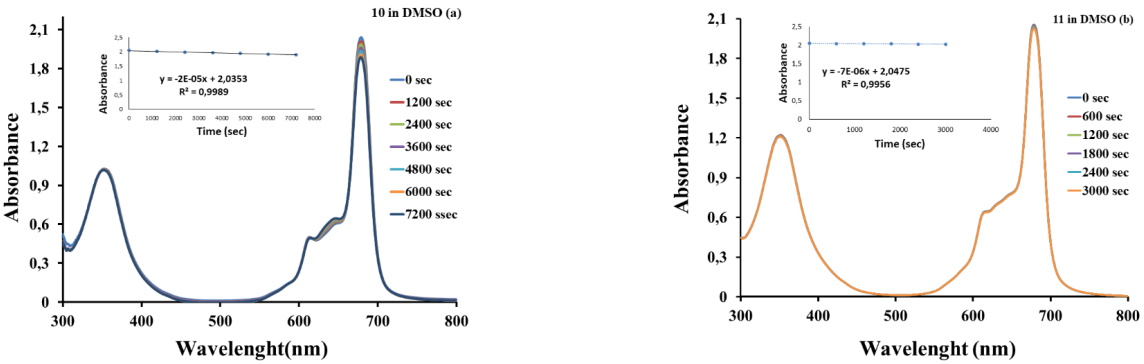

Figure 6. A typical spectrum for the determination of photodegradation quantum yield of complexes **10** (a) and **11** (b) in DMSO.

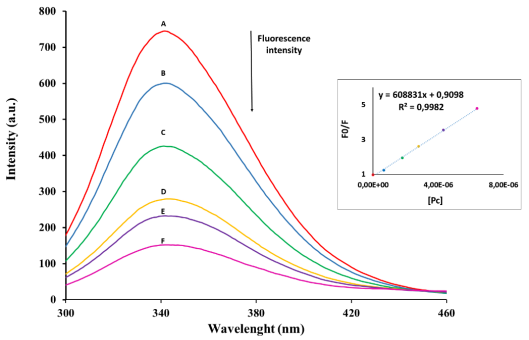

Figure 7. Fluorescence emission spectral changes of BSA [*BSA*] = 3.00×10^{-5} M with the addition of different concentrations of **11** in PBS [**11**].: A = 0, B = 6.6×10^{-7}, C = 1.80×10^{-6},
D = 2.80×10^{-6}, E = 4.30×10^{-6}, F = 8.64×10^{-6} M.

Table 3. The binding and fluorescence quenching results for the interaction of BSA with complex **11** in PBS.

Compound	K_{sv} (10^5 M^{-1})	k_q (10^{13} M^{-1} s^{-1})
11	6.08	6.08

4. Conclusion

In this study, a novel Schiff base substituted phthalocyanine complex (**9** and **10**) carrying pyridine moieties and its water-soluble quaternized derivative (**11**) were synthesized and characterized. In the synthesis of targeted Pcs, phthalocyanine compound with aldehyde functional group, which is suitable for Schiff base reaction by various primary amines, was chosen as the starting material. Photophysical and photochemical measurements showed that the Schiff base substituted derivative containing pyridine moieties did not affect the singlet oxygen production value in DMSO, but increased in DMF.

When the effect of quaternization on these properties was examined in DMSO and water containing TX-100 for PDT applications, it was determined that quaternized phthalocyanine (**11**) had effective photophysical and photochemical properties related to photosensitization, gave more important values in DMSO.

As a result of the study to define the stability of the Pc molecule under light irradiation, it was determined that the newly synthesized phthalocyanine compounds (**10** and **11**) used in solvent systems (DMSO and DMF for **10**, DMSO, and water-containing TX-100 for **11**) have suitable photodegradation stability.

The interactions between BSA and the quaternized zinc phthalocyanine (**11**) were also investigated in this study. The result of the fluorescence quenching studies of BSA presented that the water-soluble quaternized zinc phthalocyanine complex (**11**) showed strong binding to serum albumin and was easily transferable in blood. Consequently, all these results displayed that the novel ZnPc **10** and notably its water-soluble form **11** can be acceptable candidates for PDT of cancer treatment.

Acknowledgements

This study was supported by Yıldız Technical University (project no: 2016-01-02-DOP05)

References

1. Wöhrle D, Schnurpfeil G, Makarov S, Suvora O. Phthalocyanine. Chemie in Unserer Zeit 2012; 46 (1): 12-24. doi: 10.1002/ciuz.201200548
2. Özçelik Ş, Koca A, Gül A. Synthesis and electrochemical investigation of phthalocyanines with dendritic bulky ethereal substituents. Polyhedron 2012; 42 (1): 227-235. doi: 10.1016/j.poly.2012.05.025
3. Leznoff C.C. ve Lever AB. Phthalocyanines: Properties and Applications. New York: VCH Publisher, 1989.
4. Barrett PA, Dent CE, Linstead RP. 382. Phthalocyanines. Part VII. Phthalocyanine as a co-ordinating group. A general investigation of the metallic derivatives Journal of the Chemical Society 1936; 1719-1736. doi: 10.1039/jr9360001719
5. Dini D, Hanack M. Physical Properties of Phthalocyanine-based Materials. In Kadish K M, Simith K M, Guilard R (editors). The Porphyrin Handbook: Phthalocyanines: Properties and Materials. Tubingen, Germany: Elsevier Inc., 2003, 1-36.
6. De La Torre G, Vázquez P, Agulló-López F, Torres T. Phthalocyanines and related compounds: Organic targets for Nonlinear Optical applications Journal of Materials Chemistry 1998; 8 (8): 1671-1683. doi: 10.1039/a803533d
7. De la Torre G, Vázquez P, Agulló-López F, Torres T. Role of Structural Factors in the Nonlinear Optical Properties of Phthalocyanines and Related Compounds. Chemical Reviews 2004; 104 (9): 3723-3750. doi: 10.1021/cr030206t
8. Martínez-Díaz MV, de la Torre G, Torres T. Lighting porphyrins and phthalocyanines for molecular photovoltaics. Chemical Communications 2010; 46 (38): 7090. doi: 10.1039/c0cc02213f
9. Maya EM, Snow AW, Shirk JS, Pong RGS, Flom SR et al. Synthesis, aggregation behavior and nonlinear absorption properties of lead phthalocyanines substituted with siloxane chains. Journal of Materials Chemistry 2003; 13 (7): 1603. doi: 10.1039/b301566a
10. Makarov NS, Rebane A, Drobizhev M, Wolleb H, Spahni H. Optimizing two-photon absorption for volumetric optical data storage. Journal of the Optical Society of America B 2007; 24 (8): 1874-1885. doi: 10.1364/JOSAB.24.001874
11. Martín-Gomis L, Fernández-Lázaro F, Sastre-Santos Á. Advances in phthalocyanine-sensitized solar cells (PcSSCs). Journal of Materials Chemistry A 2014; 2 (38): 15672-15682. doi: 10.1039/c4ta01894j
12. Yu L, Shi W, Lin L, Guo Y, Li R et al. Asymmetric zinc phthalocyanines with large steric hindrance as efficient red/near-IR responsive sensitizer for dye-sensitized solar cells. Dye and Pigments 2015; 114: 231-238. doi: 10.1016/j.dyepig.2014.11.017
13. Kerp HR, Van Faassen EE. Effects of oxygen on exciton transport in zinc phthalocyanine layers. Chemical Physics Letters 2000; 332 (1-2): 5-12. doi: 10.1016/S0009-2614(00)01227-6
14. Blochwitz J, Pfeiffer M, Fritz T, Leo K. Low voltage organic light emitting diodes featuring doped phthalocyanine as hole transport material. Applied Physics Letters 1998; 73 (6): 729-731. doi: 10.1063/1.121982
15. Gardner JW, Iskandarani MZ, Bott B. Effect of electrode geometry on gas sensitivity of lead phthalocyanine thin films. Sensors Actuators B Chemical 1992; 9 (2): 133-142. doi: 10.1016/0925-4005(92)80206-d

16. Kong S, Wang X, Bai L, Song Y, Meng F. Multi-arm ionic liquid crystals formed by pyridine-mesophase and copper phthalocyanine. Journal of Molecular Liquids 2019; 288: 111012. doi: 10.1016/j.molliq.2019.111012

17. Gaul C, Hutsch S, Schwarze M, Schellhammer KS, Bussolottiet F et al. Insight into doping efficiency of organic semiconductors from the analysis of the density of states in n-doped C60 and ZnPc. Nature Materials 2018; 17 (5): 439-444. doi: 10.1038/s41563-018-0030-8

18. Basova T, Jushina I, Gürek A., Ahsen V, Ray A. Use of the electrochromic behaviour of lanthanide phthalocyanine films for nicotinamide adenine dinucleotide detection. Journal of The Royal Society Interface 2008; 5 (24): 801-806. doi: 10.1098/rsif.2007.1241

19. Matsuzaki K, Hiromura T, Amii H, Shibata N. Trifluoroethoxy-Coated Phthalocyanine Catalyzes Perfluoroalkylation of Alkenes under Visible-Light Irradiation. Molecules 2017; 22 (7): 1130. doi: 10.3390/molecules22071130

20. Nann T, Ibrahim SK, Woi P-M, Xu S, Ziegler J et al. Water Splitting by Visible Light: A Nanophotocathode for Hydrogen Production. Angewandte Chemie International Edition 2010; 49 (9): 1574-1577. doi: 10.1002/anie.200906262

21. Oliveira LT, Garcia GM, Kano EK, Tedesco AC, Mosqueira VCF. HPLC-FLD methods to quantify chloroaluminum phthalocyanine in nanoparticles, plasma and tissue: Application in pharmacokinetic and biodistribution studies. Journal of Pharmaceutical and Biomedical Analysis 2011; 56 (1): 70-77. doi: 10.1016/j.jpba.2011.04.016

22. Rai P, Mallidi S, Zheng X, Rahmanzadeh R, Mir Y. Development and applications of photo-triggered theranostic agents. Advanced Drug Delivery Reviews 2010; 62 (11): 1094-1124. doi: 10.1016/j.addr.2010.09.002

23. Güzel E, Günsel A, Bilgiçli AT, Atmaca GY, Erdoğmuş A et al. Synthesis and photophysicochemical properties of novel thiadiazole-substituted zinc (II), gallium (III) and silicon (IV) phthalocyanines for photodynamic therapy. Inorganica Chimica Acta 2017; 467: 169-176. doi: 10.1016/j.ica.2017.07.058

24. Dumoulin F, Durmuş M, Ahsen V, Nyokong T. Synthetic pathways to water-soluble phthalocyanines and close analogs. Coordination Chemistry Reviews 2010; 254 (23-24): 2792-2847. doi: 10.1016/j.ccr.2010.05.002

25. Dilber G, Durmuş M, Kantekin H. Non-aggregated zwitterionic Zinc(II) phthalocyanine complexes in water with high singlet oxygen quantum yield. Dyes and Pigments 2019; 160: 267-284. doi: 10.1016/j.dyepig.2018.08.019

26. Baygu Y, Gök Y. A highly water-soluble zinc(II) phthalocyanines as potential for PDT studies: Synthesis and characterization. Inorganic Chemistry Communications 2018; 96:133-138. doi: 10.1016/j.inoche.2018.08.004

27. Shaw E, Bernstein J, Losee K, Lott WA. Analogs of Aspergillic Acid. IV. Substituted 2-Bromopyridine-N-oxides and Their Conversion to Cyclic Thiohydroxamic Acids. Journal of the American Chemical Society 1950; 72 (10): 4362-4364. doi: 10.1021/ja01166a008

28. da Silva CM, da Silva DL, Modolo LV, Alves RB, de Resende M. Schiff bases: A short review of their antimicrobial activities. Journal of Advanced Research 2011;2 (1): 1-8. doi: 10.1016/j.jare.2010.05.004

29. Kantar C, Mavi V, Baltaş N, Islamoğlu F, Şaşmaz S. Novel zinc(II)phthalocyanines bearing azo-containing schiff base: Determination of pKa values, absorption, emission, enzyme inhibition and photochemical properties. Journal of Molecular Structure 2016; 1122: 88-99. doi: 10.1016/j.molstruc.2016.05.055

30. Pişkin M, Canpolat E, Öztürk ÖF. The new zinc phthalocyanine having high singlet oxygen quantum yield substituted with new benzenesulfonamide derivative groups containing schiff base. Journal of Molecular Structure 2020; 1202: 127181. doi: 10.1016/j.molstruc.2019.127181

31. Sen P, Yildiz SZ, Atmaca GY, Erdoğmuş A. Synthesis, photophysics, and photochemistry of peripherally Schiff base-zinc complex substituted zinc phthalocyanine. Journal of Coordination Chemistry 2018; 71 (8): 1258-1267. doi: 10.1080/00958972.2018.1455094

32. Şahal H, Pişkin M, Organ GA, Öztürk ÖF, Kaya M et al. Zinc(II) phthalocyanine containing Schiff base containing sulfonamide: synthesis, characterization, photophysical, and photochemical properties. Journal of Coordination Chemistry 2018; 71 (22): 3763-3775. doi: 10.1080/00958972.2018.1524140

33. Carter DC, Ho JX. Structure of serum albumin. Advances in Protein Chemistry 1994; 45: 153-203. doi: 10.1016/S0065-3233(08)60640-3.

34. Peters T. Serum albumin. Advances in Protein Chemistry 1985; 37: 161-245. doi: 10.1016/s0065-3233(08)60065-0

35. Sen P, Dege N, Yildiz SZ. Tri-nuclear phthalocyanine complexes carrying N/O donor ligands as hydrogen peroxide catalysts, and their bleaching activity measurements by an online spectrophotometric method. Journal of Coordination Chemistry 2017; 70 (16): 2751-2770. doi: 10.1080/00958972.2017.1360490

36. Nelson SM, Knox CV, McCann M, Drew MGB. Metal-ion-controlled transamination in the synthesis of macrocyclic Schiff-base ligands. Part 1. Reactions of 2,6-diacetylpyridine and dicarbonyl compounds with 3,6-dioxaoctane-1,8-diamine. Journal of the Chemical Society, Dalton Transactions 1981; (8): 1669. doi: 10.1039/dt9810001669

37. Lever, ABP., Leznoff CC. Phthalocyanines: Properties and Applications. Nex York: VCH Publications, New York.; 1996.

38. Anderson AB, Gordon TL, Kenney ME. Electronic and redox properties of stacked-ring silicon phthalocyanines from molecular orbital theory. Journal of the American Chemical Society 1985; 107 (1):192-195. doi: 10.1021/ja00287a034

39. Durmuş M, Erdoğmuş A, Ogunsipe A, Nyokong T. The synthesis and photophysicochemical behaviour of novel water-soluble cationic indium(III) phthalocyanine. Dyes and Pigment. 2009; 82 (2): 244-250. doi: 10.1016/j.dyepig.2009.01.008

40. Engelkamp H, Nolte RJM. Molecular materials based on crown ether functionalized phthalocyanines. Journal of Porphyrins and Phthalocyanines 2000; 04 (05): 454-459. doi: 10.1002/1099-1409(200008)4:5<454::aid-jpp261>3.0.co;2-d

41. Dominguez DD, Snow AW, Shirk JS, Pong RGS. Polyethyleneoxide-capped phthalocyanines: limiting phthalocyanine aggregation to dimer formation. Journal of Porphyrins and Phthalocyanines 2001; 05 (07): 582-592. doi: 10.1002/jpp.365

42. Erdoğmus A, Nyokong T. Synthesis of zinc phthalocyanine derivatives with improved photophysicochemical properties in aqueous media. Journal of Molecular Structure 2010; 977 (1-3):26-38. doi: 10.1016/j.molstruc.2010.04.048

43. Nyokong T. Effects of substituents on the photochemical and photophysical properties of main group metal phthalocyanines. Coordination Chemistry Reviews. 2007; 251 (13-14): 1707-1722. doi: 10.1016/j.ccr.2006.11.011

44. Moeno S, Nyokong T. Solvent and central metal effects on the photophysical and photochemical properties of peripherally tetra mercaptopyridine substituted metallophthalocyanines. Journal of Photochemistry and Photobiology A: Chemistry 2009; 203 (2-3): 204-210. doi: 10.1016/j.jphotochem.2009.01.021

45. Ogunsipe A, Maree D, Nyokong T. Solvent effects on the photochemical and fluorescence properties of zinc phthalocyanine derivatives. Journal of Molecular Structure 2003; 650 (1-3): 131-140. doi: 10.1016/S0022-2860(03)00155-8

46. Ogunsipe A, Chen J-Y, Nyokong T. Photophysical and photochemical studies of zinc(II) phthalocyanine derivatives—effects of substituents and solvents. New Journal of Chemistry 2004; 28 (7): 822-827. doi: 10.1039/b315319c

47. Bronner C, Baudron SA, Hosseini MW, Strassert CA, Guenet A et. al. Dipyrrin based luminescent cyclometallated palladium and platinum complexes. Dalton Transactions 2010; 39 (1): 180-184. doi: 10.1039/b908424j

48. Maree SE, Nyokong T. Syntheses and photochemical properties of octasubstituted phthalocyaninato zinc complexes. Journal of Porphyrins and Phthalocyanines 2001; 05 (11): 782-792. doi: 10.1002/jpp.388

49. Peng Y, Huang F, Wen J, Huang B, Ma X et al. A spectroscopic study of the interaction of octacarboxylic metal phthalocyanine with bovine serum albumin. Journal of Coordination Chemistry 2008; 61 (10): 1503-1512. doi: 10.1080/00958970701655561

50. Al-Raqa SY, Khezami K, Kaya EN, Durmuş M. A novel water soluble axially substituted silicon(IV) phthalocyanine bearing quaternized 4-(4-pyridinyl)phenol groups: Synthesis, characterization, photophysicochemical properties and BSA/DNA binding behavior. Polyhedron. 2021; 194: 114937. doi: 10.1016/j.poly.2020.114937

51. Çakir V, Çakir D, Pişkin M, Durmuş M, Biyiklioğlu Z. Water soluble peripheral and non-peripheral tetrasubstituted zinc phthalocyanines: Synthesis, photochemistry and bovine serum albumin binding behavior. Journal of Luminescence 2014; 154: 274-284. doi: 10.1016/j.jlumin.2014.04.030

52. Çolak S, Durmuş M, Yildiz SZ. The water-soluble zwitterionic and cationic tetra-substituted zinc(II) phthalocyanines: Synthesis, photophysical, photochemical and protein binding properties. Polyhedron. 2016; 113: 115-122. doi: 10.1016/j.poly.2016.04.026

53. Çakir V, Çakir D, Pişkin M, Durmuş M, Biyiklioğlu Z. New peripherally and non-peripherally tetra-substituted water soluble zinc phthalocyanines: Synthesis, photophysics and photochemistry. Journal of Organometallic Chemistry 2015; 783: 120-129. doi: 10.1016/j.jorganchem.2015.02.021

54. Chauke V, Ogunsipe A, Durmuş M, Nyokong T. Novel gallium(III) phthalocyanine derivatives – Synthesis, photophysics and photochemistry. Polyhedron. 2007; 26 (12): 2663-2671. doi: 10.1016/J.POLY.2007.01.016

Supplementary Information

1. Materials and equipment

Dimethylsulfoxide (DMSO), 1-pentanol, methanol, n-hexane, chloroform ($CHCl_3$), tetrahydrofuran (THF), acetone, K_2CO_3, ethanol, and dimethylformamide (DMF), dichloromethane (DCM), $NaHCO_3$, Na_2SO_4 were purchased from Merck, 1,8-diazabicyclo[5.4.0]undec-7-ene (DBU), 1,3-diphenylisobenzofuran (DPBF), 9,10-antrasendil-bis (metilen) dimalonoik asit (ADMA), 4-hydroxybenzaldehyde, 4-nitrophthalonitrile, ethylene glycol, $FeCl_3.6H_2O$ zinc acetate, zinc phthalocyanine ZnPc), tetrasulfonated zinc phthalocyanine (ZnTSPc), acetic acid were purchased from Sigma Aldrich. Column chromatography was performed on silica gel 60 (0.04–0.063 mm).

FT-IR spectra (KBr pellets) were measured with a Perkin Elmer Spectrum One Spectrometer. Absorption spectra in the UV-visible region were obtained with a Shimadzu 2001 UV spectrophotometer.

Fluorescence spectra were done using a Varian Eclipse spectrofluorometer using 1 cm pathlength cuvettes at room temperature. ^{1}H NMR spectra were recorded in D_2O (water soluble zinc phthalocyanine) and DMSO-d_6 (metal free and zinc phthalocyanine) solutions on a Varian 500 MHz spectrometer.

Photo-irradiations were done using a General Electric quartz line lamp (300 W). A 600 nm glass cut off filter (Schott) and a water filter were used to filter off ultraviolet and infrared radiations respectively. An interference filter (Intor, 700 nm with a bandwidth of 40 nm) was additionally placed in the light path before the sample. Light intensities were measured with a POWER MAX5100 (Molelectron detector incorporated) power meter. The mass spectra were acquired on a Bruker Daltonics (Bremen, Germany) MicroTOF mass spectrometer equipped with an electrospray ionization (ESI) source. The instrument was operated in positive ion mode using a m/z range of 50–3000. The capillary voltage of the ion source was set at 6000 V and the capillary exit at 190 V. The nebulizer gas flow was 1 bar and drying gas flow 8 mL/min.

2. Photophysical and photochemical studies

2.1. Fluorescence quantum yields

Fluorescence quantum yields (Φ_F) were determined by the comparative method (Eq. 1) [S1],

$$\Phi_F = \Phi_{F(Std)} \frac{F \,.\, A_{Std} \,.\, n^2}{F_{Std} \,.\, A \,.\, n^2_{Std}} \tag{1}$$

where F and F_{Std} are the areas under the fluorescence emission curves of the samples and the standard, respectively. A and A_{Std} are the respective absorbances of the samples and standard at the excitation wavelengths, respectively. n^2 and n^2_{Std} are the refractive indices of solvents used for the sample and standard, respectively. Unsubstituted ZnPc (in DMSO) (Φ_F = 0.20) [S2], (in DMF) (Φ_F = 0.17) [S3], was employed as the standard. Both the samples and standard were excited at the same wavelength. The absorbance of the solutions at the excitation wavelength ranged between 0.04 and 0.05.

2.2. Singlet oxygen quantum yields

Singlet oxygen quantum yield (Φ_Δ) determinations were carried out using the experimental set-up described in the literature [S5–S8]. Quantum yields of singlet oxygen photogeneration were determined in air (no oxygen bubbled) using the relative method (Eq. 2) with ZnPc as reference. 1,3-Diphenylisobenzofuran (DPBF) for organic solvent and 9,10-antracenediyl-bis(methylene)dimalonoic acid (ADMA) for aqueous solution were used as chemical quencher for singlet oxygen, using equation 2

$$\Phi_\Delta = \Phi_\Delta^{Std} \frac{R \,.\, I_{abs}^{Std}}{R^{Std} \,.\, I_{abs}} \tag{2}$$

where Φ_Δ^{Std} is the singlet oxygen quantum yields for the standard ZnPc (Φ_Δ^{Std} = 0.67 in DMSO) and Φ_Δ^{Std}=0.56 in DMF) [S8], and ZnTSPc ($\ddot{O}_\Delta^{Std}$ = 0.30 in aqueous solution in the presence of Triton X) [S9]. R and R_{Std} are the quencher photobleaching rates in the presence of the samples and standard, respectively. I_{abs} and I_{abs}^{Std} are the rates of light absorption by the samples and standard, respectively. Typically, a 3 mL portion of the respective unsubstituted ZnPc, ZnTSPc or synthesized phthalocyanines (**5**, **7**, **10,** and **11**) solutions containing the singlet oxygen quencher was irradiated in the Q band region with the photo irradiation set-up described in the references [S5,8]. To avoid chain reactions induced by the quenchers (DPBF or ADMA) in the presence of singlet oxygen, the concentration of the quenchers (DPBF or ADMA) was lowered to ~3×10^{-5} M [S10]. Solutions of the sensitizer (C = 1×10^{-5} M) containing the quencher (DPBF or ADMA) were prepared in the dark and irradiated in the Q band region. DPBF degradation at 417 nm and ADMA degradation at 380 nm were monitored. The light intensity of 1.74×10^{15} photons s^{-1} cm^{-2} was used for Φ_Δ determinations.

2.3. Photodegradation quantum yields

Photodegradation quantum yield (Φ_d) determinations were carried out using the experimental set-up described in the literature [S6–S7]. Photodegradation quantum yields were determined using formula 3,

$$\Phi_d = \frac{(C_0 - C_t) \cdot V \cdot N_A}{I_{abs} \cdot S \cdot t} \quad (3)$$

where "C_0"and "C_t" are the sample concentrations before and after irradiation respectively, "V" is the reaction volume, "N_A", the Avogadro's constant, "S", the irradiated cell area and "t", the irradiation time, "I_{abs}" is the overlap integral of the radiation source light intensity and the absorption of the samples. A light intensity of 5.35×10^{15} photons s^{-1} cm^{-2} was employed for Φ_d determinations.

3. Binding properties of quaternized zinc(II) phthalocyanine to BSA protein

The binding of quaternized zinc (II) phthalocyanine complex (**11**) to BSA was studied by spectrofluorometry at room temperature in PBS solution. The PBS of a fixed concentration of BSA (3.00×10^{-5} M) was titrated with varying concentrations of the **11** solution. BSA was excited at 280 nm and the fluorescence emission spectra were recorded between 290 and 450 nm. The steady diminution of the fluorescence emission of BSA with the increase in the **11** concentrations was recorded. The fluorescence intensity for BSA decreased by addition of the quaternized zinc (II) phthalocyanine (**11**) solutions and these reductions were related to quaternized phthalocyanine concentrations by the Stern-Volmer relationship (Equation 4):

$$\frac{F_0^{BSA}}{F^{BSA}} = 1 + K_{SV}^{BSA}[Pc] \quad (4)$$

and k_{SV}^{BSA} is given by Equation 5:

$$K_{SV}^{BSA} = k_q \tau_{F(BSA)} \quad (5)$$

where F_0^{BSA} and F^{BSA} are the fluorescence intensities of BSA in the absence and presence of quaternized phthalocyanine (**11**); K_{SV}^{BSA}, the Stern-Volmer quenching constant; k_q, the bimolecular quenching constant; and $\tau_{F(BSA)}$, the fluorescence lifetime of BSA ($\tau_{F(BSA)}$ = 10 ns) [S14-S16]. The K_{SV}^{BSA} values were obtained from the plots of F_0^{BSA}/F^{BSA} versus [Pc] and the k_q values can be determined from Equation 5.

4. Synthesis

4.1. 4-(4-formylphenoxy) phthalonitrile (2) and 4-[4-(1,3-Dioxolan-2-yl)phenoxy]phthalonitrile (3)

The preparation of **2** was carried out by reaction of 4-nitrophthalonitrile and 4-hydroxybenzaldehyde (**1**) according to the published literature [S13]. 4-[4-(1,3-Dioxolan-2-yl)phenoxy]phthalonitrile (**3**) was obtained for protecting the aldehyde group with ethylene glycol according to the published literature [S13]. The obtained spectroscopic data are in accordance with the literature.

4.2. Tetrakis[4-(1,3-dioxolan-2-yl)phenoxy]phthalocyanine (4)

4-(4-(1,3-dioxolan-2-yl)phenoxy)phthalonitrile **(3)** (800 mg, 3.42 mmol) was mixed with a catalytic amount of DBU (a couple drops) in 2.5 mL of n-pentanol. After the reaction mixture was degassed in the argon system at room temperature, the reaction temperature was increased to 140 °C. It was stirred under Ar atmosphere for 18 h at this temperature. The crude product was precipitated by adding methanol/water (1/1) mixture to the mixture cooled to room temperature. The precipitate formed **(3)** was collected by centrifugation, washed with methanol several times to dissolve any unwanted organic impurity and dried in vacuum. Yield: 2.08 g (98%). UV-vis (DMSO): $\boldsymbol{\lambda}_{max}$ nm (log ε) 700 (5.04), 669 (4.32), 350 (4.86). FT-IR $\boldsymbol{\nu}_{max}$/cm^{-1} (KBr pellet): 3288 (-NH), 3063 (Ar., C-H), 2951, 2881(Aliph., C-H), 1602–1505 (Ar., C=C), 1470–1391 (Aliph., C-C), 1221 (Asym., Ar-O-Ar), 1107 (C-O-C), 1009 (Sym, Ar-O-Ar), 925,740. ^{1}H NMR (DMSO-d6): δ = 7.33–6.64 (b, 47H, ArH), 4.88 (d, 4H), 3.90 (d, 16H), MS (MALDI-MS) m/z: Calc: 1170.121; Found: 1170.336 $[M]^+$.

4.3. Tetrakis[4-(1,3-dioxolan-2-yl)phenoxy]phthalocyaninato zinc(II) (5)

Acetal substituted phthalocyanine (800 mg, 0.648 mmol) (**4**) was dissolved in 2 mL dry n-pentanol and anhydrous Zn $(OAc)_2$ (194 mg, 0.648 mmol) was added to the reaction media. The mixture was heated at 140 °C and stirred 18 h at this temperature. After the reaction mixture was left to cool into the room temperature, n-hexane was added (30 mL) and the precipitate was filtered. The obtained spectroscopic data are in accordance with the literature [S13].

4.4. Tetrakis[4-(4-formylphenoxy)]phthalocyanine (6)

Acetal substituted phthalocyanine (800 mg, 0.648 mmol) **(4)** was dissolved in 5 mL of THF and stirred in acetic acid/ $FeCl_3.6H_2O$ (catalytic amount) for 1 day at room temperature according to the published literature [S13]. The mixture was precipitated by adding water (15 mL). The precipitate **(6)** formed was separated by centrifugation, washed with hot water, methanol and dried in a vacuum oven. Yield: 475 mg (70%). UV-vis (DMSO): $\boldsymbol{\lambda}_{max}$ nm (log ε) 700 (5.04), 669 (4.32), 350 (4.86). FT-IR $\boldsymbol{\nu}_{max}$/cm^{-1} (KBr pellet): 3287 (-NH), 3063–3035 (Ar., C-H), 2828–2735 (O=C-H), 1693 (-C=O), 1592–1500 (Ar., C=C), 1470–1394 (Aliph, C-C), 1227 (Asym, Ar-O-Ar), 1153 (Sym, Ar-O-Ar). ^{1}H NMR ($CDCl_3$): δ = 10.05–10.00 (d, 4H, O=C-H). MS (MALDI-MS) m/z: Calc: 994.108; Found: 1056.094 $[M+Na+K]^+$.

4.5. Tetrakis[4-(4-formylphenoxy)phthalocyaninato zinc(II) (7)

Aldehyde substituted phthalocyanine (800 mg, 0.758 mmol) (**6**) was dissolved in 2 mL dry n-pentanol and anhydrous $Zn(OAc)_2$ (247 mg, 0.758 mmol) was added to the reaction media. The mixture was heated at 140 °C and stirred 18 h at this temperature. After the reaction mixture was left to cool into the room temperature, n-hexane was added (30 mL) and the precipitate was filtered. The obtained spectroscopic data are in accordance with the literature [S13].

4.6. Tetrakis [4-(4-methoxybenzylidene)-1-(pyridin-4-yl) methanimin] phthalocyanine (9)

Tetrakis [(4-formylphenoxy)]-phthalocyanine (4) (200 mg, 2.02 mmol) was dissolved with 15 mL dichloromethane and 4-(aminomethyl)pyridine (**8**) (130 mg, 10 mmol) was added dropwise. After the reaction mixture was degassed in the argon system at room temperature, the reaction temperature was increased to 35 °C. It was stirred under Ar atmosphere for 20 h at this temperature. The solvent of the mixture, which was cooled to room temperature, was removed by using a 1/10 rotary system, methanol was added to the reaction vessel and the crude product was precipitated. The precipitate formed **(9)** was centrifuged, washed with methanol, and dried in a vacuum oven. Yield: 225 mg (88%). UV-vis (DMSO): λ_{max} nm (log ε) 700 (5.04), 669 (4.32), 350 (4.86). FT-IR $\boldsymbol{\nu}_{max}$/cm^{-1} (KBr pellet): 3287 (-NH), 3062–3029 (Ar., C-H), 1642 (C=N), 1596 (Ar., C=C), 1501–1396 (C-C), 1223 (Asym., Ar-O-Ar), 1090 (C-N), 1046 (Sym., Ar-O-Ar). ^{1}H NMR (DMSO-d6): δ = 8.72–8.71 (m, 4H, CH_2), 8.54–8.37 (d, 16H, ArH), 7.76–7.71 (d, 8H, ArH), 7.55 (s, 3H, ArH), 7.36–7.34 (d, 17H, ArH). MS (MALDI-MS) m/z: Calc: 1355.146; Found: 1355.288 $[M]^+$.

4.7. Tetrakis [4-(4-methoxybenzylidene)-1-(pyridin-4-yl) methanimin] phthalocyaninato zinc(II) (10)

Tetrakis [4-(4-methoxybenzylidene)-1-(pyridin-4-yl) methanimin] phthalocyanine **(9)** (180 mg, 0.12 mmol) and $Zn(OAc)_2$ (36 mg, 0.12 mmol) were mixed in 2 mL of n-pentanol. After the reaction mixture was degassed in the argon system at room temperature, the reaction temperature was increased to 140 °C. The crude product was precipitated by stirring under Ar atmosphere for 18 h at this temperature. Then, the crude product which was cooled to room temperature was precipitated by adding hexane. The precipitate formed **(10)** was centrifuged, and washed successively with cold methanol and ethanol to remove unreacted starting materials and dried in a vacuum oven. Yield: 187 mg (78%). UV-vis (DMSO): λ_{max} nm (log ε) 679 (5.00), 613 (4.24), 355 (4.48). FT-IR ν_{max}/cm^{-1} (KBr pellet): 3030 (Ar, C-H), 1643 (C=N), 1597 (Ar, C=C), 1484–1391 (C-C), 1255 (Asym, Ar-O-Ar), 1087 (C-N), 1043 (Sym, Ar-O-Ar). ^{1}H NMR (DMSO-d_6): δ = 9.04–8.95 (s, 4H, HC=N), 8.77–8.46 (m, 13H, ArH), 8,22–7.80 (m, 18H, ArH), 7.60–7.24 (m, 13H, ArH) and 4.86–4.83 (d, 8H, CH_2). MS (MALDI-MS) m/z: Calc: 1418.396; Found: 1418.105 $[M]^+$.

4.8. Tetrakis [4-(4-methoxy benzylidene)-1-(pyridin-4-yl) methanimin] phthalocyaninato zinc(II) sulfate (11)

This complex was prepared according to the method previously reported by Smith et al. [S14]. Compound **9** (155 mg, 0.109 mmol) was heated to 120 °C in freshly distilled 2 mL DMF and excess dimethylsulphate (0.1 mL) was added dropwise using a micro syringe. The mixture was stirred at 120 °C for 10 h. After this time, the mixture was cooled to room temperature and the product was precipitated with hot acetone and collected by filtration. The green solid product was washed successively with acetone, ethanol, ethyl acetate, DCM, THF, chloroform, n-hexane and diethylether. The resulting hygroscopic product was dried over phosphorous pentoxide Yield: 118 mg (65%). UV-vis (DMSO): λ_{max} nm (log ε) 679 (4.89),615 (4.52), 351 (4.86). UV-vis (Water + Triton X-100): λ_{max} nm (log ε) 680 (4.03), 612 (4.38), 364 (4.26). FT-IR ν_{max}/cm^{-1} (KBr pellet): 3038 (Ar., C-H), 2959–2862 (Aliph., C-H), 1601–1469 (C=C), 1392–1334 (C-O), 1165 (Asy., S=O), 1042 (Sym., S=O), 1013, 768. ^{1}H NMR (D_2O): δ = 8.68 (s, 2H), 8.10 (s, 2H), 7.77 (d, 6H), 7.42 (d, 12H), 7.31 (d, 14H), 7.10 (d, 12H), 4.28 (s, 12H, CH_3), 3.54 (s, 12H, CH_2). MS (MALDI-MS) m/z: Calc. 1671.015; Found: 1939,192 $[M+DIT+K+3H]^+$.

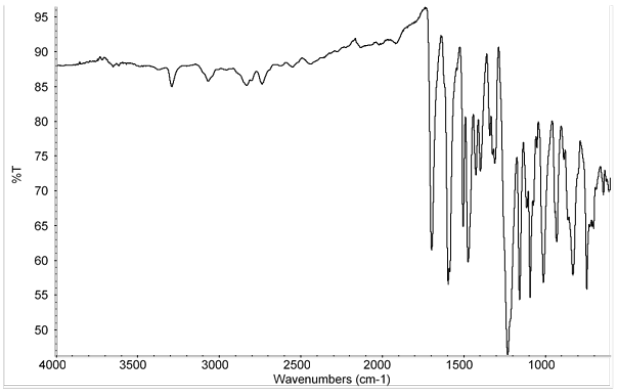

Figure S1. FT-IR spectrum of compound **4.**

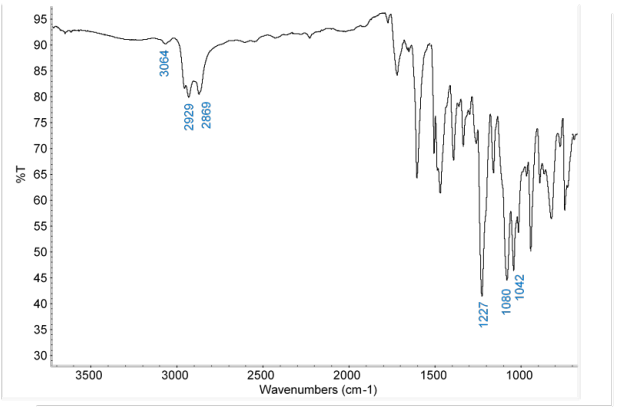

Figure S2. FT-IR spectrum of compound **5.**

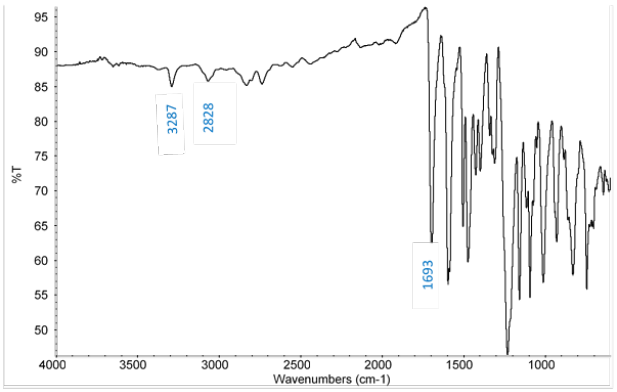

Figure S3. FT-IR spectrum of compound **6.**

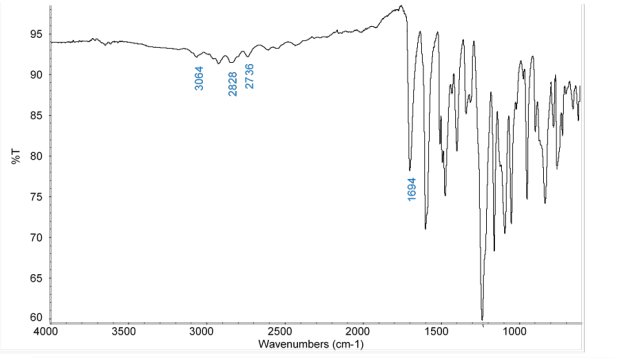

Figure S4. FT-IR spectrum of compound **7.**

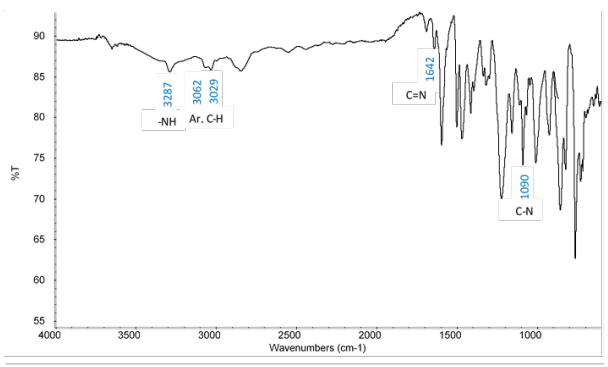

Figure S5. FT-IR spectrum of compound **9.**

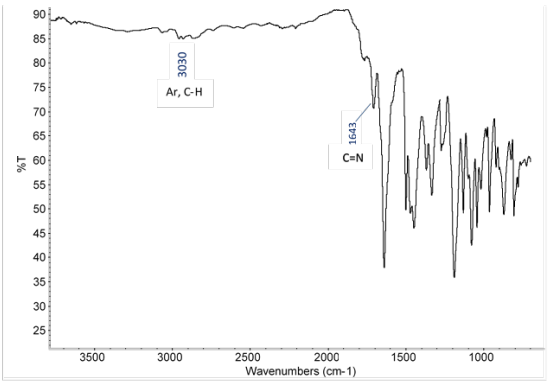

Figure S6. FT-IR spectrum of compound **10.**

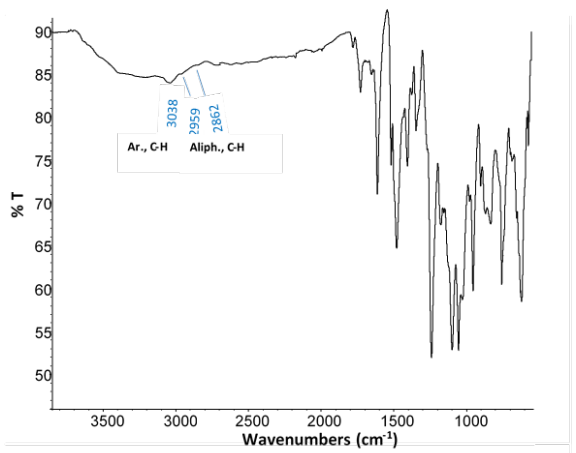

Figure S7. FT-IR spectrum of compound **11.**

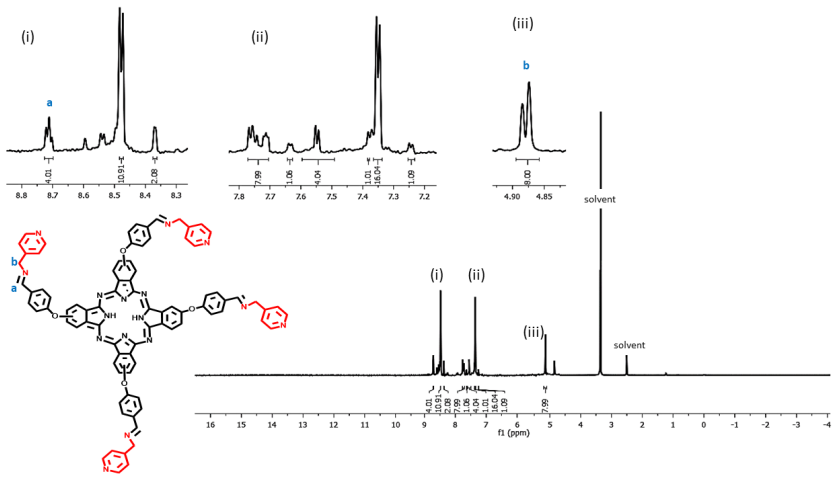

Figure S8. [1]H NMR spectrum of compound **9.**

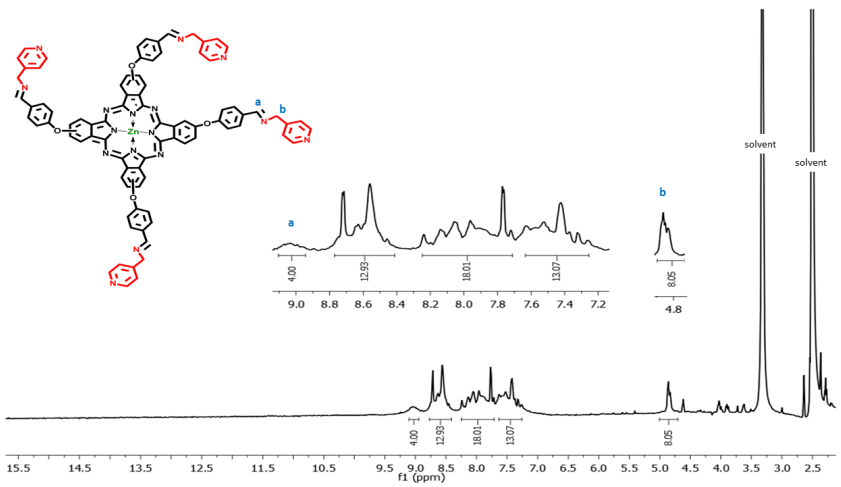

Figure S9. [1]H NMR spectrum of compound **10.**

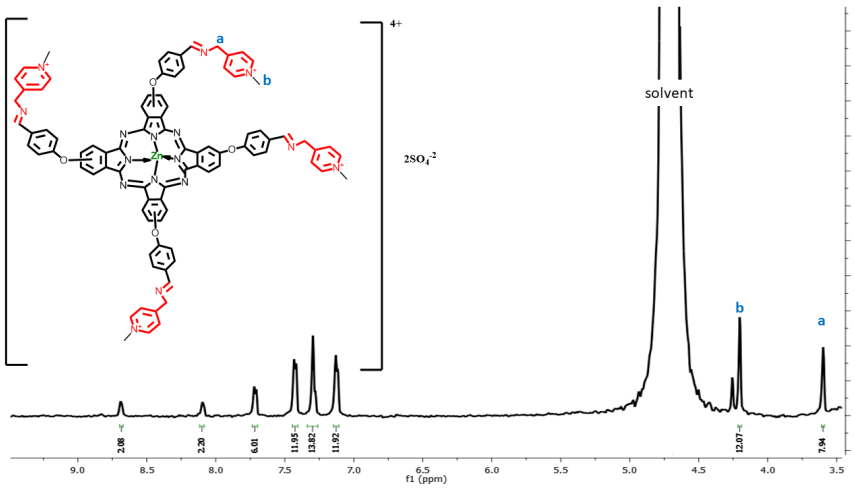

Figure S10. ^{1}H NMR spectrum of compound **11.**

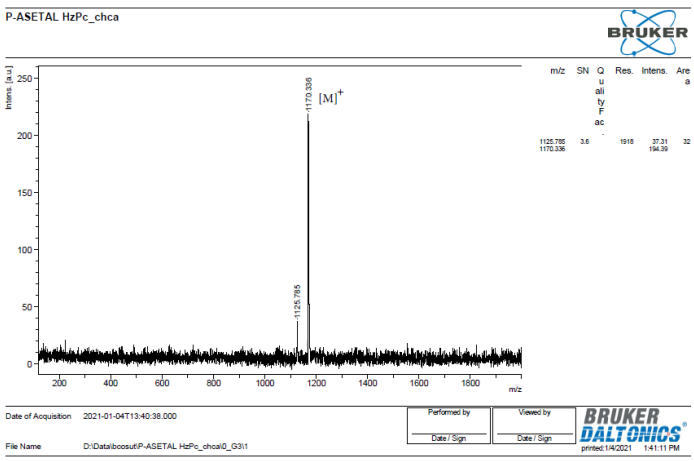

Figure S11 (a). MALDI TOF MS spectrum of compound **4.** (The molecular ion peak value of the fragmentation product $(M\text{-}C_2H_6O]^+$:1125.785)

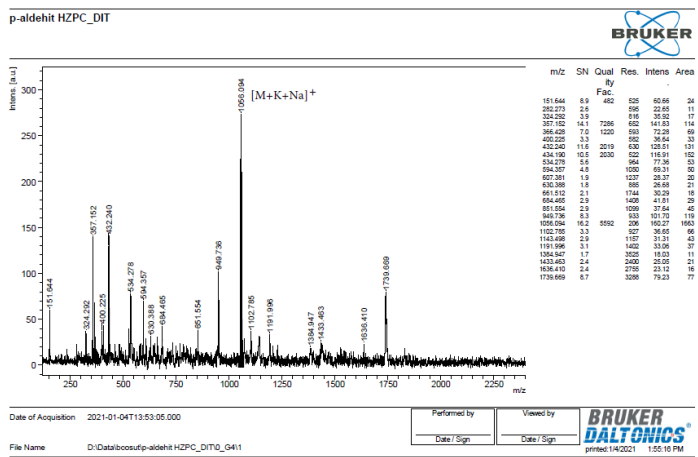

Figure S11 (b). MALDI TOF MS spectrum of compound **6.** (The molecular ion peak value of the fragmentation product $(M\text{-}2(CHO)+10H]^+$: 949.736).

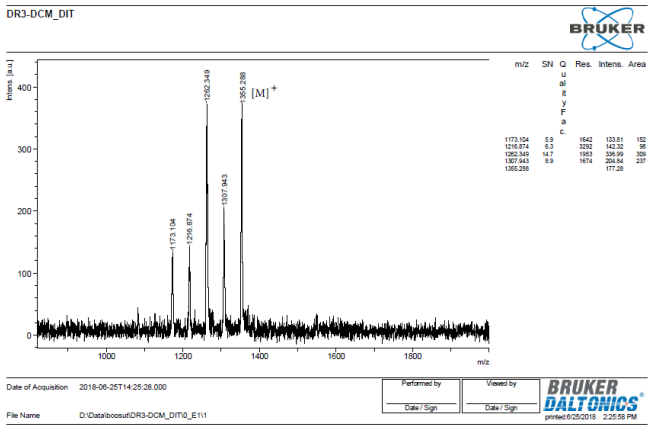

Figure S11 (c). MALDI TOF MS spectrum of compound **9** (The molecular ion peak value of the fragmentation product $[M-(C_7H_9N)]^+$: 1262.349 and $([M-2(C_7H_9N)]^+$:1173.104).

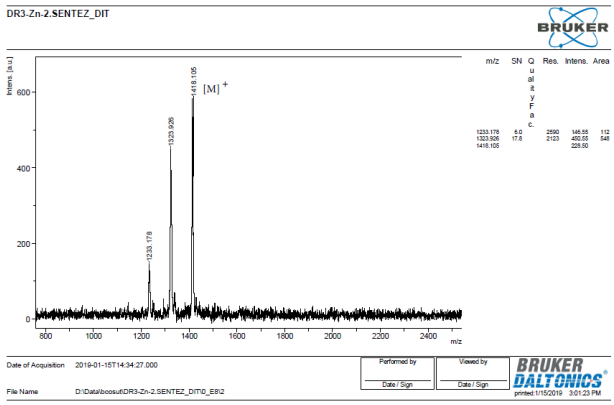

Figure S11 (d). MALDI TOF MS spectrum of compound **10** (The molecular ion peak value of the fragmentation product $[M-(C_7H_9N)+2H)]^+$: 1323.926 and $([M-2(C_7H_9N)]^+$:1233.178).

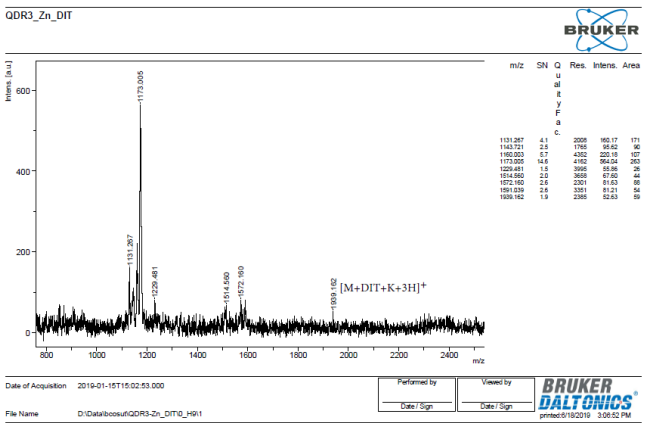

Figure S11 (e). MALDI TOF MS spectrum of compound **11** (The molecular ion peak value of the fragmentation product $[M-(C_{25}H_3S_2O_8N_3)+Na+H]^+$: 1173.005.

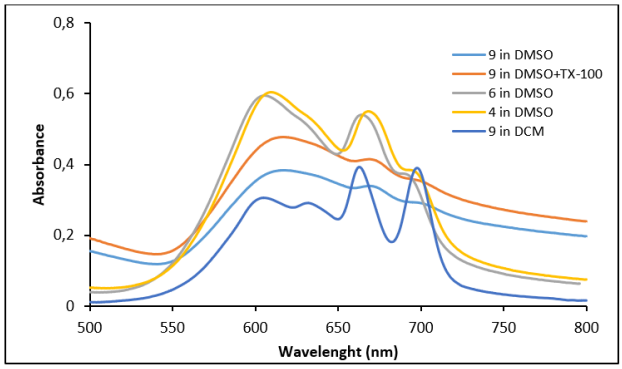

Figure S12. UV-vis absorption spectra of metal-free phthalocyanines **4**, **6**, and **9** in different solvents (amount of addition of Triton X-100: 0.1 mL in DMSO).

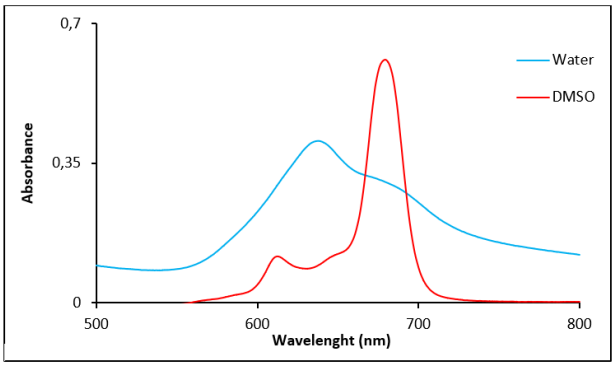

Figure S13. UV-vis absorption spectra of complex **11** in water ([11]=1.0 × 10^{-6} M)
and DMSO ([11] = 6.0 × 10^{-6} M).

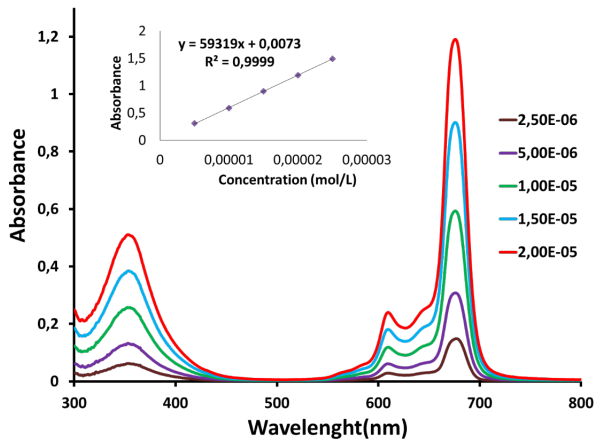

Figure S14. Absorption spectra of complex **10** at different concentrations in DMF.

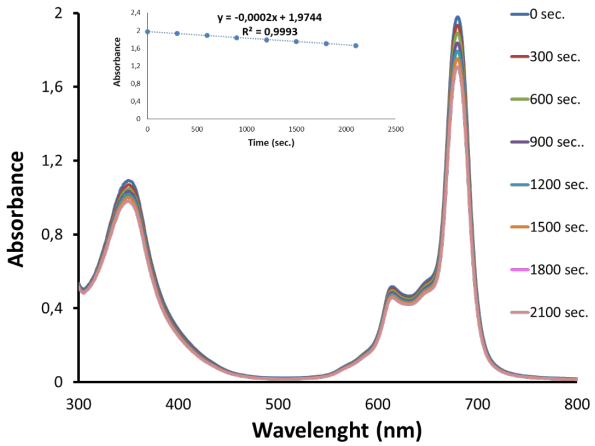

Figure S15. A typical spectrum for the determination of photodegredation. This figure was for complex **11**in 0.1 mL TX-100 added water (initial [**11**]= 24 × 10^{-6} M).

References

S1. Frey-Forgues S, Lavabre D. Are fluorescence quantum yields so tricky to measure? A demonstration using familiar stationery products. Journal of Chemical Education 1999; 76: 1260-1264. doi: 10.1021/ed076p1260

S2. Ogunsipe A, Chen JY, Nyokong T. Photophysical and photochemical studies of zinc(II) phthalocyanine derivatives effects of substituents and solvents. New Journal of Chemistry 2004; 25: 822-827. doi: 10.1039/B315319C

S3. Durmus M, Nyokong T. Photophysicochemical and fluorescence quenching studies of benzyloxyphenoxy-substituted zinc phthalocyanines. Spectrochim Acta A. 2008; 69: 1170-1177. doi: 10.1016/j.saa.2007.06.029

S5. Brannon JH, Madge D. Picosecond laser Photophysics. group 3A phthalocyanines. Journal of the American Chemical Society 1980;102: 62-65

S6. Ogunsipe A, Nyokong T. Photophysical and photochemical studies of sulphonated non-transition metal phthalocyanines in aqueous and non-aqueous media. Journal of Photochemistry and Photobiology A: Chemistry 2005; 173: 211-220. doi: 10.1016/j.jphotochem.2005.03.001

S7. Seotsanyana-Mokhosi I, Kuznetsova N, Nyokong T. Photochemical studies of tetra-2,3-pyridinoporphyrazines. Journal of Photochemistry and Photobiology A: Chemistry 2001; 140: 215-222. doi:10.1016/j.jphotochem.2005.03.001

S8. Ogunsipe A, Maree D, Nyokong T. Solvent effects on the photochemical and fluorescence properties of zinc phthalocyanine derivatives. Journal of Molecular Structure 2003; 650: 131-140. doi: 10.1016/S0022-2860(03)00155-8

S9. Masilela N, Idowu M and Nyokong T. Photophysical, photochemical and electrochemical properties of water soluble silicon, titanium and zinc phthalocyanines, J. Photochem. Photobiol. A Chem., 2009; 201: 91–97. doi: 10.1016/j.jphotochem.2008.10.009

S10. Spiller W, Kliesch H, Wöhrle D, Hackbarth S, Roder B et al. J. Porphyr. Phthalocyanines, Singlet Oxygen Quantum Yields of Different Photosensitizers in Polar Solvents and Micellar Solutions, 1998; 145: 145-158. doi: 10.1002/(SICI)1099-1409(199803/04)2:2<145::AID-JPP60>3.0.CO;2-2

S11. Çakir V., Çakir D., Pişkin M., Durmuş M., and Biyiklioğlu Z. Water soluble peripheral and non-peripheral tetrasubstituted zinc phthalocyanines: Synthesis, photochemistry and bovine serum albumin binding behavior, J. Lumin., 2014; 154: 274–284. doi: 10.1016/j.jlumin.2014.04.030

S12. Jiang C. Q., Gao M. X., He J. X. Study of the interaction between terazosin and serum albumin -Synchronous fluorescence determination of terazosin, Anal. Chim. Acta, 2002; 452: 185–189.

S13. Sen P., Dege N., Yildiz S. Z., Tri-nuclear phthalocyanine complexes carrying N/O donor ligands as hydrogen peroxide catalysts,and their bleaching activity measurements by anonline spectrophotometric method, J. Coord. Chem., 2018; 70: 2751–2770. doi: 10.1080/00958972.2017.1360490

S14. Smith T. D., Livorness J., Taylor H., Pilbrow J. R., Sinclair G.R., Physico-chemical study of copper(II) and cobalt(II) chelates of tetra-2,3-pyridinoporphyrazine, J. Chem. Soc. Dalton Trans., 1983; 7: 1391–400. doi: 10.1039/DT9830001391